Learning autonomous vehicle passengers' preferred driving styles using g-g plots and haptic feedback

Kalabic, U.; Chakrabarty, A.; Quirynen, R.; Di Cairano, S.

TR2019-115 October 18, 2019

Abstract

In this work, we present and experimentally validate a framework for learning an autonomous vehicle passenger's preferred driving style. The study is performed with N = 3 human subjects in a vehicle simulator that consists of a 3-DOF motion simulator, providing feelings of longitudinal and lateral acceleration to the passenger, an automatically controlled steering wheel, providing information about the steering controller behavior, and a computer monitor, providing a virtual rendering of the view through the windshield. The vehicle controller is designed to track speeds while satisfying limits on the maximum allowable longitudinal and lateral accelerations. These accelerations are related to the passenger's preferences and are represented as a surface on a g-g plot. The passenger's preferences are learned from comfort labels provided by the passenger, which correspond to positive and negative assessments of the vehicle's current driving behavior. In the framework that we present, these labels directly change the corresponding parametrization of the g-g plot, thereby modifying the limiting constraints to be enforced by the controller on-line, which leads to a change in the behavior of the vehicle. The collected data supports the hypothesis that there is a personalized driving style preference, and also shows that our proposed preference-learning scheme converges to a preferred driving style.

IEEE Intelligent Transportation Systems Conference (ITSC)

Learning autonomous vehicle passengers' preferred driving styles using g-g plots and haptic feedback

Uroš Kalabić Ankush Chakrabarty Rien Quirynen Stefano Di Cairano

***Abstract*— In this work, we present and experimentally validate a framework for learning an autonomous vehicle passenger's preferred driving style. The study is performed with $N = 3$ human subjects in a vehicle simulator that consists of a 3-DOF motion simulator, providing feelings of longitudinal and lateral acceleration to the passenger, an automatically controlled steering wheel, providing information about the steering controller behavior, and a computer monitor, providing a virtual rendering of the view through the windshield. The vehicle controller is designed to track speeds while satisfying limits on the maximum allowable longitudinal and lateral accelerations. These accelerations are related to the passenger's preferences and are represented as a surface on a g-g plot. The passenger's preferences are learned from comfort labels provided by the passenger, which correspond to positive and negative assessments of the vehicle's current driving behavior. In the framework that we present, these labels directly change the corresponding parametrization of the g-g plot, thereby modifying the limiting constraints to be enforced by the controller on-line, which leads to a change in the behavior of the vehicle. The collected data supports the hypothesis that there is a personalized driving style preference, and also shows that our proposed preference-learning scheme converges to a preferred driving style.**

I. INTRODUCTION

As vehicles with autonomous capabilities become more widely available to the general public, it becomes important to consider the interaction between these vehicles and their human users. One aspect of interaction is the identification of a preferred driving style, one of whose purposes is the customization or modification of vehicle behavior to a user's preferences. To this end the majority of research has considered the replication of human driving styles, both inside and outside the context of autonomy. There are two directions to this research. The focus of the first direction has been the categorization of driving styles into coarse behavioral clusters such as calm, normal, and aggressive [1] to be able to select one of these clusters as a user's preferred driving style. The focus of the second has been the conversion of driving style into control policies; attempts have used various technical approaches, including input-output autoregressive models [2], time-varying state-space models [3], hidden Markov models [4], Gaussian mixture models [5], neural networks [6], [7], and inverse reinforcement learning [8], [9].

The commonality between all these methods is that they seek to replicate a driver's style when the vehicle operates in autonomous mode. However, this misses the realization that, *when a vehicle is driving autonomously, the human in the driving seat is not a driver, but a passenger*. Instead of replicating the driving style associated with the driver's behavior as driver, it may be better for the design to replicate the preferred style of the driver as passenger. In [10], researchers tested the hypothesis whether users of autonomous vehicles would truly want the vehicle to replicate their own driving, concluding that users would prefer a more defensive style than their own. In fact, the work concluded that most people were not capable of categorizing their own driving style into even coarse behavioral clusters.

Therefore, there is a need to determine a representation of driving behavior that is adequate for use in a closed-loop vehicle controller and can be determined using learning methods. In this work, we propose that *passenger preference learning*, or *driver-as-passenger driving style learning*, can be performed by learning the limiting accelerations on a g-g plot based on user feedback. The utility of g-g plots, also referred to as traction circles, is established in the vehicle dynamics literature. According to [11], the g-g plot is "representative of a comfortable operating region for the driver" and provides a rational method for estimating driver style under different road and environmental conditions. More recently, [12] has demonstrated the effectiveness of g-g plots in estimating safety margins and user preferences in assisted driving settings. Employing the g-g plot for constrained control of vehicles has been investigated in [13] for cornering a vehicle at tire friction limits, in [14] for restoring stability after sharp and aggressive maneuvers, and in [15] for adding robustness to parametric uncertainties such as tire stiffness variations while controlling mobile robots.

In this work, we learn a g-g plot by obtaining user feedback and use the plot to inform a control scheme which enforces the acceleration constraints. To this end, we run a pilot study consisting of human-in-the-loop experiments using a motion simulator capable of replicating vehicle motions during acceleration, deceleration, and turning maneuvers. We simulate the driving environment using CarSim and Simulink in order to replicate realistic driving in a safe environment. Binary labels of comfort are provided by subjects via buttons on the hardware interface. These labels automatically reshape the envelope of g-g plot over multiple laps until our learning algorithm converges on a g-g plot that is deemed comfortable by the subject.

The use of simulation environments for understanding human-vehicle interactions is well-established [16]. For example, experiments made to study cognitive load while driving in [17], with a simple hardware-in-the-loop driver

This work was supported by Mitsubishi Electric Research Laboratories.
The authors are with Mitsubishi Electric Research Laboratories, Cambridge, MA 02139, USA. E-mails: {kalabic,chakrabarty, quirynen,dicairano}@merl.com

simulator, were shown to map closely to drivers' cognitive loads in the real world. Furthermore, three-dimensional vehicle and communication simulators have been demonstrated to be excellent precursors to on-road testing in [18], [19] while providing insights into potential improvements and adjustments for real-world use. A simulated environment is important in learning passenger preference, as it allows us to determine the limits of our methodology without endangering test subjects.

The results of our experiments show that it is possible to learn the limits of an autonomous vehicle passenger's preferred driving style using feedback from the passenger. We find evidence that a passenger has a personalized driving style when traveling in an autonomous vehicle and that this driving style can be identified by modifying the parameters of the vehicle controller. Since the g-g plot is intrinsic to our control and preference-learning scheme, we conclude that it is effective in representing the preferred driving style of an autonomous vehicle passenger.

II. Vehicle Dynamics and Control

In this section, we present the control architecture which we have implemented for determination of passenger preference.

A. Longitudinal and lateral control

For longitudinal vehicle control, we consider the model $m\dot{v}_x = F_x - R_x$, from [20], where v_x is the longitudinal vehicle speed, F_x is the force on the vehicle center of mass by the controller and R_x is the sum of all reaction forces. We assume that there is no slip in the transmission so that the engine speed ω_e is equal to the transmission shaft speed ω_t, which is linearly related to the vehicle speed via some inertia I_e, that is, $I_e\omega_e = v_x$. For this reason, we design a proportional controller to track a desired vehicle speed $v_{d,x}$, that is, $\tau_e = -K_p(v_x - v_{d,x})$, where τ_e is the torque acting on the engine. We therefore obtain the closed-loop dynamics $\dot{v}_x = -(K_p/I_e m)(v_x - v_{d,x}) - R_x$. According to these closed-loop dynamics, we observe that setting K_p large enough will enable the controller to closely track the desired velocity.

For lateral vehicle control, we consider the single-track error-tracking model proposed in [20] for a constant longitudinal speed v_x, which is given by,

$$\dot{e} = A_e e + B_\delta \delta + B_{\dot{\psi}} \dot{\psi}_d, \tag{1}$$

with $e \triangleq \begin{bmatrix} e_y & \dot{e}_y & e_\psi & \dot{e}_\psi \end{bmatrix}^\top$. Here, e_y is the lateral displacement of the vehicle position from the reference path, e_ψ is the difference between actual and desired vehicle yaw angles, δ is the front wheel angle, and $\dot{\psi}_d$ is the desired vehicle yaw rate. The system matrices are given by

$$A_e = \begin{bmatrix} 0 & 1 & 0 & 0 \\ 0 & -\frac{2C_0}{mv_x} & \frac{2C_0}{m} & -\frac{2C_1}{mv_x} \\ 0 & 0 & 0 & 1 \\ 0 & -\frac{2C_1}{I_z v_x} & \frac{2C_1}{I_z} & -\frac{2C_2}{I_z v_x} \end{bmatrix},$$

$$B_\delta = \begin{bmatrix} 0 \\ \frac{2C_{\alpha,f}}{m} \\ 0 \\ \frac{2\ell_f C_{\alpha,f}}{I_z} \end{bmatrix}, \; B_{\dot{\psi}} = \begin{bmatrix} 0 \\ -\frac{2C_1}{mv_x} - v_x \\ 0 \\ -\frac{2C_2}{I_z v_x} \end{bmatrix},$$

with coefficients $C_0 = C_{\alpha,f} + C_{\alpha,r}$, $C_1 = \ell_f C_{\alpha,f} - \ell_r C_{\alpha,r}$, $C_2 = \ell_f^2 C_{\alpha,f} + \ell_r^2 C_{\alpha,r}$. Other relevant system parameters include the longitudinal vehicle speed v_x, the vehicle mass m, the moment of inertia about the vertical I_z, the front and rear tire stiffness $C_{\alpha,f/r}$, and the distance from the vehicle ℓ_f, ℓ_r for the front and rear axles, respectively. We assume that the desired yaw rate $\dot{\psi}_d = 0$.

We design a gain-scheduled controller for the system (1) for regulating the desired longitudinal speed $v_{d,x}$. Specifically, we design a set of state-feedback gains K_{v_x} for $v_x \in V_x = \{5, 10, \ldots, 150\}$km/h. The road wheel angle is set to, $\delta = -K_{v_{d,x}} e$. where $K_{v_{d,x}}$ is the linearly-interpolated value between the nearest gains K_{v_x} corresponding to the desired vehicle velocity $v_{d,x}$. Specifically, $K_{v_{d,x}} = K_{v_{d,x}^-} + \frac{v_{d,x} - v_{d,x}^-}{v_{d,x}^+ - v_{d,x}^-} K_{v_{d,x}^+}$, where, $v_{d,x}^- = \max\{v_x \in V_x : v_x \leq v_{d,x}\}$ and $v_{d,x}^+ = \min\{v_x \in V_x : v_x > v_{d,x}\}$.

B. Model of passenger preference using g-g plots

We assume that a passenger's comfort preferences are related to the coupling between longitudinal and lateral accelerations that he feels while riding in a vehicle. Specifically, we assume that the limits of comfort adhere to the following relationship,

$$\begin{cases} \left|\frac{a_x}{a_{\max}}\right|^p + \left|\frac{a_y}{c_{\max}}\right|^p \leq 1, & \text{if } a_x \geq 0, \\ \left|\frac{a_x}{b_{\max}}\right|^p + \left|\frac{a_y}{c_{\max}}\right|^p \leq 1, & \text{if } a_x < 0, \end{cases} \tag{2}$$

where a_x and a_y are the longitudinal and lateral accelerations felt by the passenger, $a_{\max}$, $b_{\max}$, and $c_{\max}$ are the maximum magnitudes of positive longitudinal acceleration, negative longitudinal deceleration, and lateral acceleration, respectively, and $p \in (0, 2]$ is a parameter relating longitudinal and lateral accelerations.

C. Performing maneuvers to test preferences

We aim to experimentally identify a passenger's internal comfort region, that is, his personalized parameters $a_{\max}$, $b_{\max}$, $c_{\max}$, and p. To do this, we perform a sequence of alternating maneuvers in a simulated track environment. The track we have designed for this purpose is plotted in Fig. 1. In the plot, the track is labeled by type of maneuver being tested. There are four maneuvers: A, B, C, and P, which test $a_{\max}$, $b_{\max}$, $c_{\max}$, and p, respectively.

In all maneuvers, the experimental procedure simply varies the desired velocity $v_{d,x}$ along the track, according to a procedure designed to reach the expected limits of passenger comfort. In the following, we describe each maneuver.

1) Maneuvers A and B: To begin, we describe the maneuvers that are designed to test a passenger's acceleration and deceleration limits. These are performed on the three straight segments of the track. During Maneuver A, the vehicle speeds up at the maximum allowable acceleration

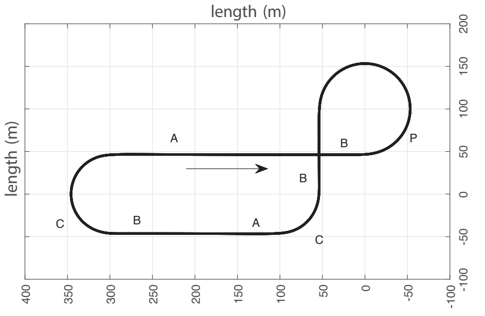

Fig. 1. Plot of track with direction of travel and labeled maneuvers.

$a_{\max}$. During Maneuver B, the vehicle slows down at the maximum allowable deceleration $b_{\max}$. This is accomplished by varying the desired velocity $v_{d,x}$ so that, if the vehicle tracks the velocity perfectly, the required acceleration or deceleration will be achieved.

To determine the desired velocity, we assume that there is an initial velocity v_i near the beginning of the straight segment and a final, exit velocity v_f near the end. Given a passenger's maximum acceleration $a_{\max}$, we can compute the velocity profile that adheres to a constant acceleration set at $a_{\max}$ in terms of length along the road segment $s - s_0$. This velocity profile is given by,

$$v_{d,+}(s) = \sqrt{v_i^2 + 2a_{\max}(s - s_0)}. \tag{3a}$$

Similarly, given a passenger's maximum deceleration $b_{\max}$, we can compute the velocity profile that adheres to a constant deceleration set at $b_{\max}$ in terms of length away from the end of the road segment $s_f - s$. This velocity profile is given by,

$$v_{d,-}(s) = \sqrt{v_f^2 + 2b_{\max}(s_f - s)}. \tag{3b}$$

In general, the initial velocity v_i is set to the desired velocity at which the vehicle exits the curve preceding the straight-line segment; the final velocity v_f is set to the desired velocity at which the vehicle enters the next curve.

Between maneuvers A and B, the velocity is set to $v_{\max} = 33$m/s. To ensure consistency between the three choices of velocity, we take the minimum of the three when traveling along the straight segment, *i.e.*, the longitudinal velocity is set to the minimum of the maximum velocity and the velocities computed by (3), that is, $v_{d,x}(s) = \min\{v_{d,+}(s), v_{d,-}(s), v_{\max}\}$.

2) Maneuver C: To test the lateral acceleration, we drive the vehicle through the curves at a constant velocity. Since the curved segments of the track are circular arcs, the acceleration on the vehicle is constant. Using the expression for centripetal acceleration, the desired speed is set to $v_{d,x} = \sqrt{r_1 c_{\max}}$, where r_1 is the radius of curvature of the turn during both segments.

3) Maneuver P: In the final maneuver, we test a passenger's preferred relationship between longitudinal and lateral acceleration. To do this, we set the desired velocity so that the curve on the g-g plot will follow the periphery of the boundary (2). To solve for the required velocity, we begin by assuming that $a_x = \dot{v}_{d,x}$ and $a_y = v_{d,x}^2/r_2$, where r_2 is the radius of curvature of the turn. Since the turn is left handed, we obtain the differential equation,

$$(\dot{v}_{d,x}/a_{\max})^p + (v_{d,x}^2/r_2 c_{\max})^p = 1. \tag{4}$$

Since the desired velocity $v_{d,x}$ is a function of distance along the path s, we note that $\dot{s} = v_x \approx v_{d,x}$ and perform a change of variables to obtain the differential equation,

$$\left(\frac{v'_{d,x}}{a_{\max}}\right)^p + \left(\frac{v_{d,x}}{r_2 c_{\max}}\right)^p = \frac{1}{v_{d,x}^p}, \; v'_{d,x} = \frac{dv_{d,x}}{ds}, \tag{5}$$

which we solve with initial condition $v_{d,x} = 0.1\sqrt{r_2 c_{\max}}$ over the 250m length of the segment, and for values $p = 0.2, 0.4, \ldots, 2$.

D. Learning preferences from passenger feedback

During the experiment, passengers are asked for their opinion on the vehicle behavior during every maneuver, and their responses are limited to *yes* or *no*.

The learning procedure is the same for Maneuvers A, B, and C. Without loss of generality, let y^k represent one of $a_{\max}$, $b_{\max}$, or $c_{\max}$. During the corresponding maneuver, *i.e.*, A, B, or C, respectively, we set,

$$y^{k+1} = \begin{cases} \min(y^k + \Delta y^k, y^k_{\max}) & \text{if "yes"}, \\ \max(y^k - \Delta y^k, y^k_{\min}) & \text{if "no"}, \\ y^k & \text{otherwise}. \end{cases} \tag{6}$$

The variables $y^k_{\min}$ and $y^k_{\max}$ are the minimum and maximum values corresponding to the appropriate maneuver. The variable Δy^k represents the step-size corresponding to the appropriate maneuver. It is set to the smaller of the maximum step-size allowed and the golden ratio $\gamma \approx 0.618$ of the difference between $y^k_{\max}$ and $y^k_{\min}$, that is, $\Delta y^k = \min\{\gamma(y^k_{\max} - y^k_{\min}), \Delta y_{\max}\}$. The maximum and minimum values are determined according to the logic that, if the passenger provides an opposite response to his previous response, he has reached a limit. Specifically,

$$y^{k+1}_{\min} = \begin{cases} y^k & \text{if "yes" at } k \text{ and "no" at } k-1, \\ y^k_{\min} & \text{otherwise}, \end{cases}$$

$$y^{k+1}_{\max} = \begin{cases} y^k & \text{if "no" at } k \text{ and "yes" at } k-1, \\ y^k_{\max} & \text{otherwise}. \end{cases}$$

The response at $k = -1$ is assumed to be null.

The learning procedure for p^k is as follows. At the beginning of the experiment, we set $p^0 = 2$ and, during Maneuver P, we modify p^k according to the responses from the passenger,

$$p^{k+1} = \begin{cases} \max\{p^k - 0.2, 0.2\} & \text{if "no" at } k, \\ p^k & \text{otherwise}. \end{cases}$$

In this way p^k is always decreasing until it reaches the value of 0.2. This choice is guided by the assumption that a passenger has a fixed comfort region and that the initial conditions for $a_{\max}$, $b_{\max}$ and $c_{\max}$ are well within limits. Therefore, at the beginning of the experiment, a value of $p^0 = 2$ will ensure that the region satisfying (2) will be within the true comfort region and will only start pushing against boundaries as the simulation progresses. Furthermore, our assumption implies that, once boundaries are reached, p^k can only decrease. We use a different method when exploring for p^k compared with the other parameters because a difference of less than 0.2 is not large enough to make a material difference in the behavior of Maneuver P.

E. Experimental setup and subjects

The experiment is performed in an environment that combines hardware elements with a virtual driving simulator, a schematic of which is provided in Fig. 2. The vehicle dynamics are simulated using CarSim 2018.0 and the control architecture is implemented using MATLAB Simulink R2015b. The road visualization and speedometer are provided via the CarSim VS Visualizer and projected onto a computer monitor with 60Hz refresh rate. A signal is sent from Simulink over UDP to a separate computer, which runs the software used to actuate a D-BOX GP PRO-200 motion simulator. The simulator has been modified, with its original gaming wheel replaced with a Thrustmaster T300RS gaming wheel. The gaming wheel is controlled by Simulink to track the direction of the front wheel angles. The gaming wheel is mounted on a stationary base with two buttons, which are used for passenger feedback.

The D-BOX motion simulator provides three degrees of motion: roll, pitch, and heave, along with chair vibration. We control simulator motions by sending the value of the corresponding signal from CarSim via Simulink and UDP to the motion control software. For roll, pitch, and heave, the motion control software passes the motions through a high-pass filter to attenuate the DC values. Because of this, the motion controller removes any steady-state roll, pitch, or heave position. We relate the simulator vibration to the vehicle's actual longitudinal speed v_x, where the minimum vibration corresponds to the initial v_i and the maximum vibration corresponds to the maximum $v_{d,x}$ achieved during a maneuver. Note that these values change at the initiation of every maneuver.

During the experiment, participants sit in the motion simulator, *i.e.*, chair, and look forward at the computer screen, which shows the vehicle driving through a city track and a predicted vehicle path represented with blue dots. An example of what a participant sees is given in Fig. 2, in the "driver perspective" window. During each maneuver, participants are asked whether they liked the particular motion. Specifically, during Maneuver A, they are asked "Did you like the acceleration?" During Maneuver B: "Did you like the braking?" During Maneuver C: "Did you like the turning?" During Maneuver P: "Did you like the acceleration through the curve?" They respond to these questions by pressing one of two buttons on the gaming wheel base, with the left button indicating "yes" and the right button indicating "no." The response is received by Simulink, which updates the learned parameters and the control logic in an online, human label-driven manner.

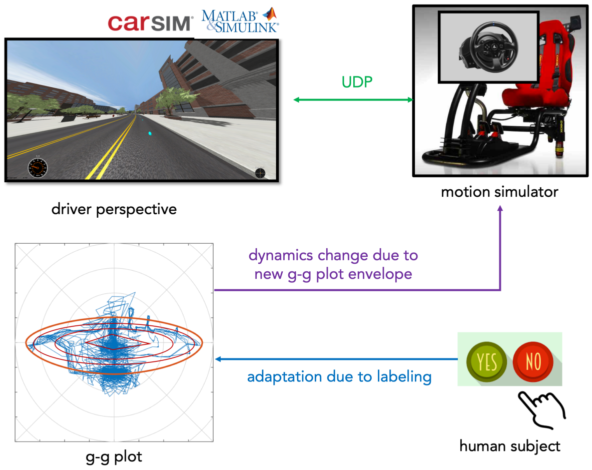

Fig. 2. Schematic of experimental setup.

The subjects included 2 male adults and 1 female adult, from an age range of 25–35. Subjects were first shown the track in Fig. 1, and each component of the experimental setup was explained. The algorithm was not explained to avoid biasing. The only directive given to each subject was to label whether they would feel comfortable in the current driver style setting for an extended period of time. It was clarified that their objective was to determine a comfortable, as opposed to tolerable, setting. All human subject experiments were approved by the Institutional Review Board (IRB) at Mitsubishi Electric Research Laboratories, Cambridge, MA.

F. Controller performance

In this section, we present the performance of our control scheme as it relates to the experiment. Specifically, we show that the longitudinal controller can accurately track desired velocity set-points along the driving path and that this results in an appropriate corresponding vehicle acceleration. To do this, we perform one lap around the track with parameters set constant at $a_{\max} = 2$ m/s^2, $b_{\max} = 3$ m/s^2, $c_{\max} = 3$ m/s^2, and $p = 1$.

In Fig. 3, we show the achieved velocity and acceleration trajectories corresponding to the test run. The results show that the longitudinal controller tracks the desired velocity. The plots also show that, as required for the experiment, the longitudinal acceleration achieves close to its desired value during the first and third time that Maneuver A is performed, that the deceleration achieves close to its desired value whenever Maneuver B is performed, and that the lateral acceleration achieves close to its desired value whenever Maneuvers C and P are performed.

III. Results and Discussion

In this section, we present the results of our experimental study. In Fig. 4, we present the evolution of the parameters a^k, b^k, c^k, and p^k and their corresponding minimum and maximum values. The parameters are plotted against the

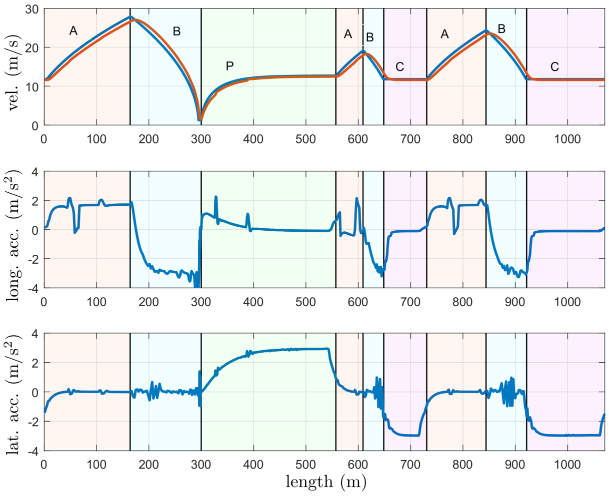

Fig. 3. Results corresponding to one lap around the track, with desired (blue) and actual (red) longitudinal velocity (top), longitudinal acceleration (middle), and lateral acceleration (bottom); transitions between maneuvers are demarcated by black vertical lines and shading and maneuvers are labeled in the top plot.

number of total maneuvers performed. The experiments were performed until it was deemed that each subject's labeled inputs had sufficiently converged. The experiments lasted 580.9 s, 716.9 s, and 698.2 s, for subject #1 through #3, respectively. At the end of the experiment, each subject converged to a set of parameters, the representation of which is plotted in Fig. 5, overlaying a plot of the trace showing acceleration applied to the vehicle center of gravity.

It is evident from the results that there is a strong dependency between the acceleration parameters (a, b, and c) and subjects' perceptions of the corresponding acceleration haptics. For our small cohort size, the relationship with the parameter p remains inconclusive. Subjects #1 and #2 indicated only once that they did not like the acceleration during Maneuver P. In contrast, Subject #3 exhibited the expected behavior: As the vehicle reached higher speeds due to the increase in a^k and c^k, the subject consistently lowered the value of p^k until convergence of the other parameters. After performing the experiment, we asked Subject #3 about their intention; they explained that they were looking at the speedometer and it seemed inappropriate for the vehicle to be accelerating so fast in a curve. After the experiment, Subjects #1 and #2 indicated during discussion that they had mostly ignored the readings from the speedometer. We conclude from these insights that our experimental setup was effective in emulating acceleration and deceleration on straight roads, but was limited in its capability to convey acceleration through a curve.

From the viewpoint of personalization, it is important to consider the consistency of subjects' responses. Specifically, we observed that subjects did not typically regret their responses or change their minds after labeling. From the results corresponding to the learning of a, b, and c parameters, we can see that, for most of the results, subjects would consistently reach a maximum and vary their responses around there, and thereafter converge slowly. The exception is the response pattern of Subject #2 corresponding to the lateral acceleration parameter c. The subject responded "no", indicating that a maximum had been achieved, but then proceeded to reachieve this maximum, consistently responding with a "yes" afterwards. This indicates that the subject was tolerant of a higher acceleration parameter but was not able to achieve it due to the controller setup. This result therefore suggests that it would be useful to create an algorithm with the ability to tolerate changes in perception.

Overall, the series of experiments that we performed inform us on how to better design an experiment for passenger preference learning in the future and reaffirm the need to test with larger cohorts. From the discussion above, we believe that learning preferred acceleration and deceleration on a straightaway can be done adequately on our setup. The greatest limitation to achieving the correct feelings for any motion is that the D-BOX software filters steady-state roll, pitch, and heave inputs. This means that we were not able to provide the subject a feeling of sustained acceleration. Since accelerations and decelerations on straightaways are quick maneuvers, the subjects were able to feel a sense of motion that adequately represented the accelerations. However, the feeling of lateral acceleration is proportional to the square of lateral velocity, which is sustained for longer durations; therefore, the feelings corresponding to lateral motion were less realistic. Taking into account the above discussion, it is apparent that subjects have a personalized preference associated with the parameters that were identified by the experiment. We therefore conclude that the use of g-g plot is appropriate for use in determining passenger's preference.

IV. Conclusions

In this paper, we presented a scheme for identifying passenger preferences for the driving behavior of an autonomous vehicle. In our scheme, the limits of passenger preference are represented by parameterized curves on a g-g plot. The results of our pilot experiments showed that the preferences of the subjects are personalized, and that we are able to learn these unique preference parameters using the control and learning framework used in experiment. We conclude that g-g plots are useful in determining an autonomous vehicle passenger's preferred driving style and can be integrated with control system design.

Acknowledgment

The authors thank Kenta Tominaga of Mitsubishi Electric Corporation for technical discussions.

References

[1] T. Ouali, N. Shah, B. Kim, D. Fuente, and B. Gao, "Driving style identification algorithm with real-world data based on statistical approach," SAE Technical Paper 2016-01-1422, 2016.

[2] P. Hermannstädter and B. Yang, "Identification and validation of lateral driver models on experimentally induced driving behavior," in *Proc. IEEE Int. Conf. Systems, Man, and Cybern.*, Seoul, South Korea, 2012, pp. 1165–1170.

[3] S. Di Cairano, D. Bernardini, A. Bemporad, and I. V. Kolmanovsky, "Stochastic MPC with learning for driver-predictive vehicle control and its application to HEV energy management," *IEEE Trans. Ctrl. Syst. Technol.*, vol. 22, no. 3, pp. 1018–1031, 2014.

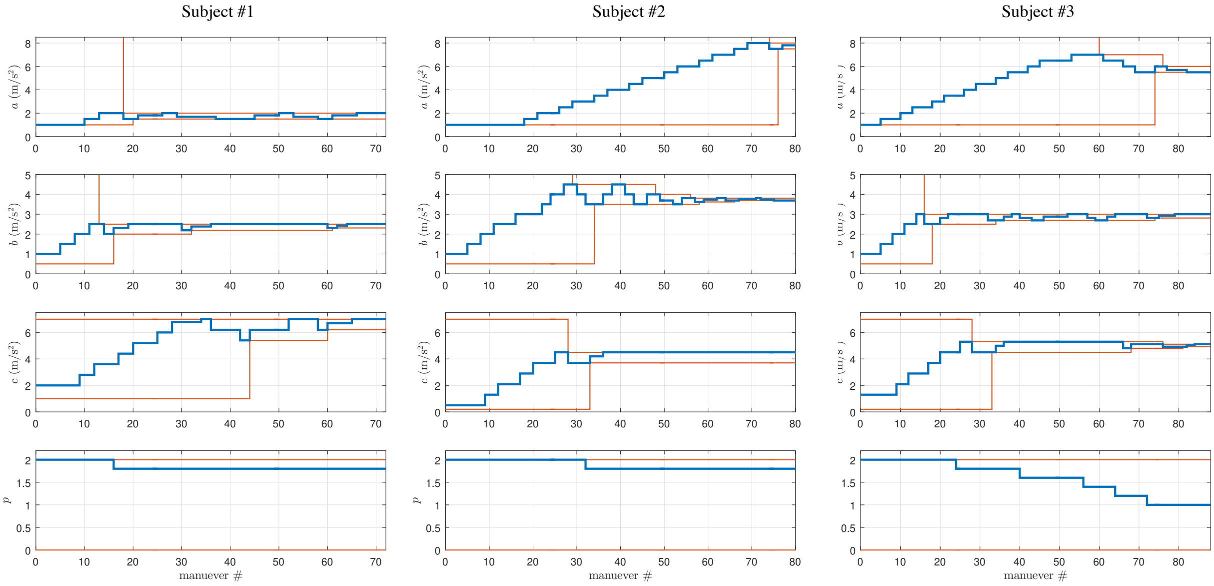

Fig. 4. Evolution of preference parameters (thick, blue) and limits (thin, red) corresponding to subjects #1–#3.

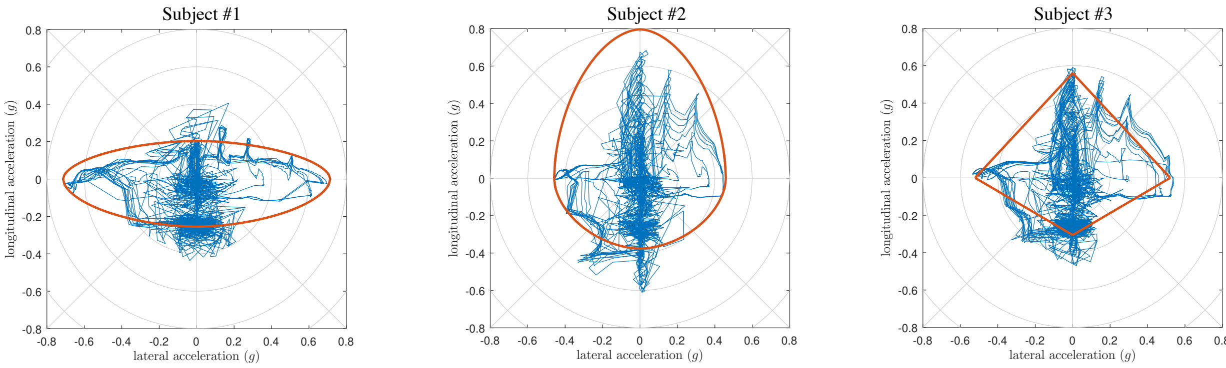

Fig. 5. Learned g-g plot (thick, red) corresponding to subjects #1–#3 with trace of acceleration applied at the vehicle's center of gravity (thin, blue).

[4] Y. Kishimoto and K. Oguri, "A modeling method for predicting driving behavior concerning with driver's past movements," in *IEEE Int. Conf. Vehic. Elec. and Safety*, Columbus, OH, 2008, pp. 132–136.

[5] D. Zhang, Q. Xiao *et al.*, "Driver curve speed model and its application to ACC speed control in curved roads," *Int. J. Auto. Tech. Kor.*, vol. 14, no. 2, pp. 241–247, 2013.

[6] A. D. Alvarez, F. S. Garcia, J. E. Naranjo, J. J. Anaya, and F. Jimenez, "Modeling the driving behavior of electric vehicles using smartphones and neural networks," *IEEE Intell. Transp. Syst. Mag.*, vol. 6, no. 3, pp. 44–53, 2014.

[7] L. Xu, J. Hu *et al.*, "Establishing style-oriented driver models by imitating human driving behaviors," *IEEE Trans. Intell. Transp. Syst.*, vol. 16, no. 5, pp. 2522–2530, 2015.

[8] M. Kuderer, S. Gulati, and W. Burgard, "Learning driving styles for autonomous vehicles from demonstration," in *Proc. IEEE Int. Conf. Robot. and Aut.*, Seattle, WA, 2015, pp. 2641–2646.

[9] J. Morton and M. J. Kochenderfer, "Simultaneous policy learning and latent state inference for imitating driver behavior," in *Intell. Transp. Syst. Conf.*, Yokohama, Japan, 2017, pp. 1129–1134.

[10] C. Basu, Q. Yang *et al.*, "Do you want your autonomous car to drive like you?" in *Proc. ACM/IEEE Int. Conf. Human-Robot Interaction*, Vienna, Austria, 2017, pp. 417–425.

[11] R. S. Rice, "Measuring car-driver interaction with the g-g diagram," SAE Technical Paper 730018, 1973.

[12] F. Biral, M. Da Lio, and E. Bertolazzi, "Combining safety margins and user preferences into a driving criterion for optimal control-based computation of reference maneuvers for an ADAS of the next generation," in *Proc. Int. Vehicles Symp.*, Las Vegas, NV, 2005, pp. 36–41.

[13] K. Kritayakirana and J. C. Gerdes, "Autonomous cornering at the limits: Maximizing a g-g diagram by using feedforward trail-braking and throttle-on-exit," in *Proc. IFAC Adv. in Automotive Ctrl.*, 2010, pp. 548–553.

[14] A. M. Daher, C. R. Bardawil, and N. A. Daher, "Vehicle stability based on g-g diagram through braking and driveline," in *Proc. American Control Conf.*, Seattle, WA, 2017, pp. 309–314.

[15] J. Ni and J. Hu, "Dynamics control of autonomous vehicle at driving limits and experiment on an autonomous formula racing car," *Mech. Syst. Signal Pr.*, vol. 90, pp. 154–174, 2017.

[16] A. L. Kun, *Human-Machine Interaction for Vehicles: Review and Outlook*. Delft, The Netherlands: Now Publishers, 2018.

[17] Y. Wang, B. Mehler *et al.*, "The validity of driving simulation for assessing differences between in-vehicle informational interfaces," *Ergonomics*, vol. 53, no. 3, pp. 404–420, 2010.

[18] F. Michaeler and C. Olaverri-Monreal, "3D driving simulator with VANET capabilities to assess cooperative systems: 3DSimVanet," in *Proc. IEEE Int. Veh. Symp.*, Redondo Beach, CA, 2017, pp. 999–1004.

[19] A. Hussein, F. García, and C. Olaverri-Monreal, "ROS and Unity based framework for intelligent vehicles control and simulation," in *Proceedings of the 2018 IEEE International Conference on Vehicular Electronics and Safety (ICVES)*. IEEE, 2018, pp. 1–6.

[20] R. Rajamani, *Vehicle Dynamics and Control*, 2nd ed. New York: Springer, 2012.